J Electr Eng Technol Vol. 8, No. 3: 565-571, 2013
http://dx.doi.org/10.5370/JEET.2013.8.3.565

ISSN(Print) 1975-0102
ISSN(Online) 2093-7423

Optimization of Energy Conversion Loop in Switched Reluctance Motor for Efficiency Improvement

Jian Li* , Ronghai Qu*, Zhichu Chen and Yun-Hyun Cho†**

Abstract – This paper presents an effective method to improve efficiency of switched reluctance motor by optimizing energy conversion loop. A nonlinear analytical model which takes saturation account is developed to calculate inductance and flux-linkage. The flux-linkage curve is studied to calculate the co-energy increment to obtain the optimum exciting current. For a given cross-section, the exciting current at which co-energy increment is maximum was found to be constant while stack length varies. Then the energy conversion loop was optimized by varying the stack length and turns of windings. The constraints during optimization were that motor was excited by the maximum increment co-energy current and the energy in the loop was determined by rated power of motor. Dynamic finite element analysis was used to evaluate the efficiency of various models and the comparison of results shows promising effects of the proposed method. Experiment was also conducted to validate the simulation result.

Keywords: Dynamic FEM simulation, Efficiency, Flux linkage, Maximum increment co-energy current, Switched reluctance motor

1. Introduction

The switched reluctance motor (SRM) has several advantages such as low cost, fault tolerance, reliability, and wide speed range at constant power. It has been widely used in variable speed drive applications such as fan, pump and electric vehicle. For energy saving purpose, efficiency improvement in electric motors has attracted much attention. Design of switched reluctance motor is a complicated procedure due to its non-linearity caused by core saturation and salient poles. Although design guides and considerations have been published in many literatures such as [1, 6], the efficiency and power density improvement and still seems to be an unsolved problem. Energy conversion loop plays an important role in the torque generation mechanism of switched reluctance motors. Energy conversion loop is of much importance to motor performance since it is determined by flux linkage and phase current, which defines the magnetic and electric loading of motor.

In this paper, a novel method is proposed to improve efficiency by optimizing energy conversion loop. The flux linkage vs. current characteristics and the corresponding energy conversion loop were first investigated for the optimum excitation current. And then the optimization was processed by varying stack length and turns of winding. The efficiency of motor with different winding configurations and stack length was studied using commercial FEM software, which can take good care of the complicated procedure of iron loss calculation.

† Corresponding Author: Dept. of Electrical Engineering, Dong-A Univerity, Korea .(yhcho@dau.ac.kr)
* State Key Laboratory of Advanced Electromagnetic Engineering and Technology, Huazhong University of Science and Technology, China. (lijian613@gmail.com)
** State Key Laboratory of Advanced Electromagnetic Engineering and Technology, Huazhong University of Science and Technology, China. (ronghaiqu@mail.hust.edu.cn)
*** Technology Center, Zhuzhou CSR Times Electric Co., Ltd., China. (chenzc@teg.cn)
Received: April 5, 2011; Accepted: December 26, 2012

2. Energy Conversion Loop and Flux Linkage Curves

Usually, rated power and the operating speed range are given by custom when designing an electric machine. These data together with dimensional constraints can be used to derive cross section dimension using equations from [3]. The motor studied in this paper has 6 stator poles and 4 rotor poles and dimensions of core are given in Appendix.

The excitation of SRM is implemented by applying a sequence of pulse current to each phase, while rotor speed is controlled by regulating current amplitude and turn on, turn off angles according to torque demand. Fig. 1 shows the typical SRM drive waveforms under single-pulse control. The corresponding energy conversion loop is illustrated in Fig. 2. The stored magnetic energy (co-energy) and the mechanical work during the 'fluxing' are $W_f + W_{md}$ and W_{mf}, respectively. The energy W_{md} is converted to mechanical work during 'de-fluxing' (diode D_1 and D_2 conduction period), and W_f is returned to the supply during the regenerative conduction period. The

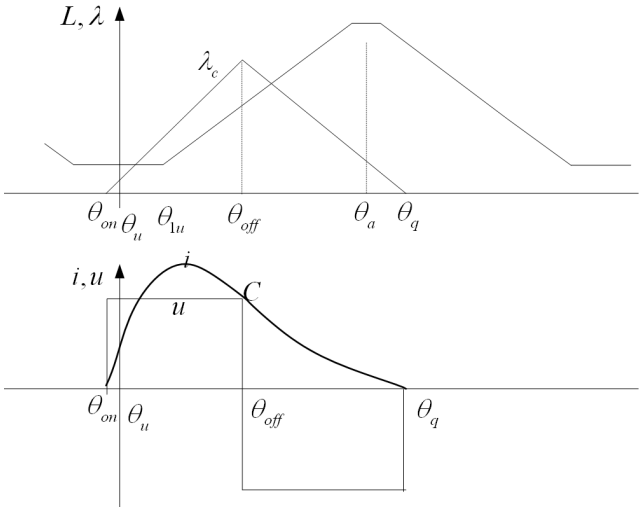

Fig. 1. Typical SRM drive waveforms under single-pulse control.

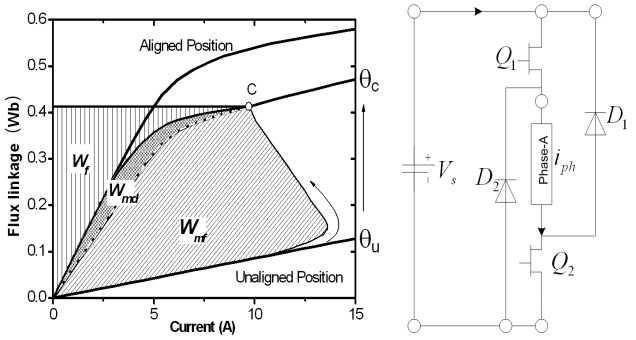

Fig. 2. Energy conversion loop of SRM in one stroke and asymmetry bridge converter for one phase

average torque is calculated as:

$$T_{av} = \frac{W_{md} + W_{mf}}{2\pi / N_r m} \tag{1}$$

where $2\pi/N_r m$ is the angle rotor obtained in one stroke and W_c is the co-energy in one stroke, N_r is the number of rotor poles, m is the number of phases. The energy that converted in one stroke is

$$W_c = W_{md} + W_{mf} \tag{2}$$

W_{mf} can be calculated by integration assuming that current is limited at I_p by chopping.

$$W_{mf} = \int_0^{I_p} (\lambda_c - \lambda_u)\, di \tag{3}$$

It's difficult to calculate the area W_{md} due to the irregular trajectory during "de-fluxing".

In order to study the flux linkage curves, a program of analytical model was developed instead of using finite element method. This model could calculate flux linkage at saturated region by interpolation of pre-defined B-H curve. The description of this method is described in detail in R. Krishnan's book [3] and also in reference [8, 9]. The accuracy of calculation method was verified by finite element analysis. Hence it's very convenient in preliminary design. The calculated flux linkage curves according to rotor positions and exciting currents are shown in Fig. 3.

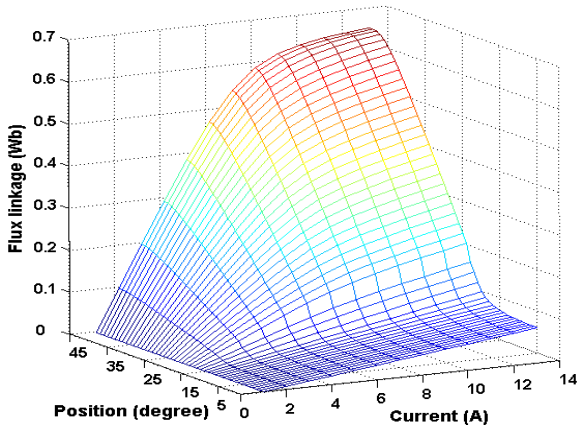

Fig. 3. 3D plot of flux linkage.

3. Optimization of Energy Conversion Loop

The energy conversion loop is composed by flux linkage curves at unaligned and commutation positions and exciting current. Area of the loop is determined by rated torque of motor and can be calculated using Eqs. (1, 2). Either increase the exciting current or the flux linkage curves will enlarge the energy conversion loop. After the cross section of motor is designed, stack length and winding determines the shape of flux linkage curves. Optimization of energy conversion loop involves three variables: exciting current, stack length and turns of winding. In this paper, the flux-linkage curve was studied first to calculate the co-energy increment to obtain the optimum exciting current. For a given cross-section, the maximum co-energy increment current was found to be constant while stack length varies. Then the energy conversion loop could be optimized by varying the stack length and turns of windings. The criterion of this procedure is that motor should be excited by the maximum increment co-energy current at rated power operation.

3.1. Maximum Co-energy Increment Current(MEIC)

It was observed from the energy conversion loop in Fig. 2 that the flux-linkage increases slightly at aligned position after saturation point but increases linearly with respect to current at unaligned position. This is because SRM is designed with a sufficiently small air gap and operated at

saturation region in order to maximize the power density at a fixed inverter volt-ampere rating [7]. The magnetic circuit is under deep saturation near aligned position and but at unaligned position magnetic circuit is far from saturation.

When taking co-energy as a variable of exciting current in Fig. 4, there is a maximum co-energy increment ΔW_c with the same increment of current ΔI. This also means that the rate of change in co-energy gets maximum value with the same increment of input current. The exciting current at which co-energy increment is maximum is defined as maximum co-energy increment current (MEIC). Excitation current should equal to or exceed MEIC to take full use of co-energy increment when designing the motor. This design criterion will be proved in the following part. The MEIC may be expressed mathematically as follows.

After obtaining the flux linkage from the analytical calculation, the curves could be described by linear and polynomial fit for unaligned and aligned position:

$$\lambda_u(i) = A_u \cdot i \tag{4}$$

$$\lambda_a(i) = B_5 \cdot i^5 + B_4 \cdot i^4 + B_3 \cdot i^3 + B_2 \cdot i^2 + B_1 \cdot i + A \tag{5}$$

Eq. (4) is a linear equation describing the flux linkage at unaligned position and the coefficient is inductance at this position. Eq. (5) is a five order polynomial which could accurately determine the nonlinear relationship between flux linkage and current.

Define

$$\begin{aligned} F(i) &= \lambda_a(i) - \lambda_u(i) \\ &= B_5 \cdot i^5 + B_4 \cdot i^4 + B_3 \cdot i^3 + B_2 \cdot i^2 + (B_1 - A_u) \cdot i + A \end{aligned} \tag{6}$$

And take derivative of it, we get

$$\frac{dF(i)}{di} = 0 \tag{7}$$

By solving Eq. (7) we can get the current I_p at which co-energy increment ΔW_C is maximum for the current increment Δi as shown in Fig. 4.

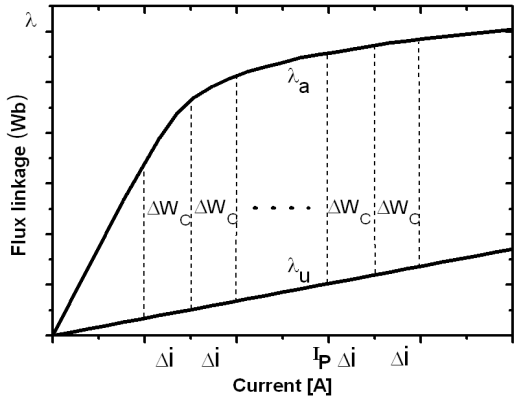

Fig. 4. Variation of co-energy increment with respect of exciting current.

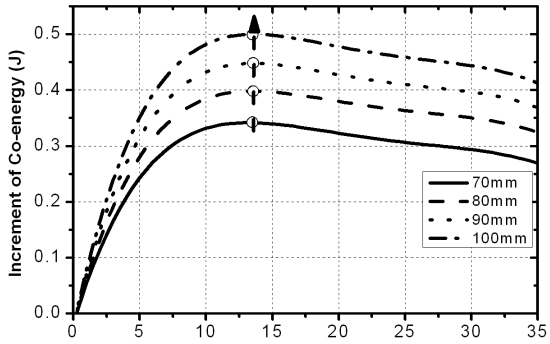

Fig. 5. Increment of co-energy with respect of the variation of phase current for different stack length.

3.2. Proper stack length according to rated torque

Here the turns of winding is constant while take the stack length as variable. The dimension of cross section is given in Appendix and the number of turns per coil is 80 turn. The MEIC is derived from Eqs. (6) and (7). The co-energy and torque are calculated by Eqs. (1) and (3). But here the co-energy converted during "de-fluxing" is not taken into account so the actual output power is larger than this calculated value.

The increment of co-energy vs. phase current at various stack lengths is illustrated in Fig. 5. The phase current increment Δi is 0.5A, and at about 13.5A, all these curves get peak value. The MEICs are almost constant in spite of stack length. This is because magnetic saturation is determined by geometry and saturation level is same for different stack length under the same electric loading. The co-energy and torque value are summarized in Table 1. It could be observed that the energy conversion loop can be optimized by varying stack length.

3.3 Turns of winding

It's observed from Table 1 that the stack length 90mm is mostly suitable to the rated torque 5.8 N.m at MEIC. In the next step, the turns of winding per stator pole increases from 60 turns to 90 turns by 10 turns per step while keeping the stack length at 90mm. The analysis results are

Table 1. Motor's output torque according to stack length

Stack Length (mm) L	Co–energy (J) W_{mf}	Torque (N.m) T_{av}
70	2.342	4.47
80	2.688	5.13
90	3.029	5.78
100	3.376	6.45

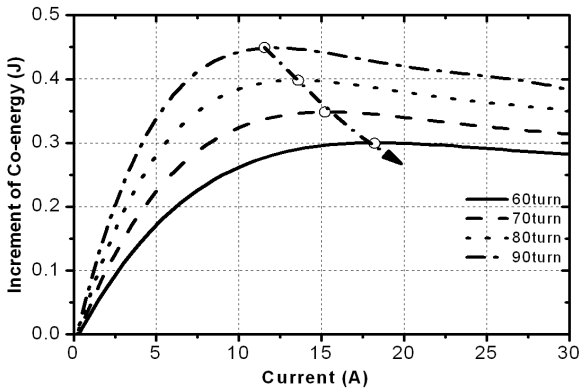

Fig. 6. Increment of co-energy with respect of the variation of phase current.

Table 2. Motor's stack length and power at MEIC

Turns per Pole	MEIC (A)	Co-energy (J)	Saturate Current (A)	Torque T_c (N.m)
60	18.1	3.1	9.03	5.81
70	15.4	3.01	7.74	5.75
80	13.5	3.08	6.52	5.78
90	12.1	3.13	5.48	5.90

given in Table 2. The saturation currents and MEICs vary while torques are near rated value for each winding design. As shown in Fig. 6, the phase current increment Δi is selected to be 0.5A, the value of MEIC increases when turns of winding decreases. The energy conversion loops with different winding and its effects on efficiency will be further studied in following sections.

4. Performance Verification and Analysis

In this section the various combinations of stack length and number of turns per pole are studied by finite element analysis (FEA).

4.1. Dynamic FEA coupling with external circuits

FEA models are developed to calculate the motor efficiency of various designs. The commercial package FLUX2D is used to model the motor and external circuits and control algorithm is developed in Matlab/Simulink. These two software could be connected by a coupling module supplied by FLUX2D. An asymmetric bridge converter with two transistors per phase is used in the external circuit. The control algorithm is developed in Matlab/Simulink, which sends gate signals to transistors in FLUX2D and receives current and position feedback signals. The turn on angle is set to obtain enough current rising time for MEIC and conducting angle is 30° during simulation. The basic theory of time-stepping FEA is given as follows. Assuming the magnetic vector potential and current density only have z-axis component, the governing

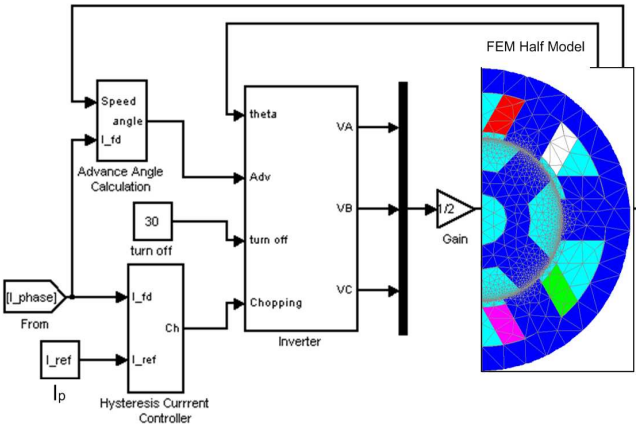

Fig. 7. Dynamic FEM simulation coupling with external circuit.

equation for SRM can be expressed in a magnetic vector potential A as follows:

$$\frac{\partial}{\partial x}(v\cdot\frac{\partial \mathbf{A}_z}{\partial x})+\frac{\partial}{\partial y}(v\cdot\frac{\partial \mathbf{A}_z}{\partial y})=-\mathbf{J} \tag{8}$$

where V is the inverse of permeability, A_z is the magnetic vector potential, and J is the input current density. The electrical input equation of the voltage source expressed as

$$V=R_s I+L_m(dI_m/dt)+E_m \tag{9}$$

where V is the voltage source, R_s is the phase resistance, L_m is the leakage inductance of the end coil, and E_m is the electromotive force induced in the coil. After applying the Galerkin method in Eq. (8) and coupling the voltage in Eq. (9), the system matrix equation is obtained by using the time difference schemes as follows:

$$\begin{bmatrix}[s] & [Q]\\ 1/\Delta t[F] & [R_s]\end{bmatrix}\begin{bmatrix}A^{t+\Delta t}\\ I_m^{t+\Delta t}\end{bmatrix}=\begin{bmatrix}0 & 0\\ 1/\Delta t[F] & 0\end{bmatrix}\begin{bmatrix}A^{t}\\ I_m^{t}\end{bmatrix}+\begin{bmatrix}0\\ V^{t+\Delta t}\end{bmatrix} \tag{10}$$

The moving line technique is introduced to carry out the dynamic analysis.

4.2. Efficiency calculation

If ventilation and friction losses are neglected, efficiency is calculated as

$$\eta=\frac{P_{Me}}{P_{Me}+P_{Cu}+P_{Fe}}=f(stack\ length, turns) \tag{11}$$

where P_{Cu} P_{Fe} P_{Me} are copper losses, iron losses and mechanical output, respectively. Accurate efficiency estimation needs more investigation on losses. The power losses in the electromechanical devices mainly have three

types: iron losses, copper losses and the mechanical losses. Copper losses can be easily calculated using phase current waveforms from simulation results,

$$P_{Cu} = mR_s \frac{1}{T}\int_0^T i(t)^2\, dt \qquad (12)$$

where m is number of phases and R_s is resistance of winding. The iron loss is calculated by LS model introduced in [10] which is based on dynamic B-H characteristics associated with transient finite element simulation. It could be more accurate comparing with the method used in [5, 8].

5. Results and Discussion

5.1. Simulation results

First the FEM models of motor with 80 turns per pole were developed and the stack length was chosen to be 70mm and 90mm respectively. The energy conversion loops and flux density along stator pole at turn off position are given in Fig. 8. The losses, electric loading and magnetic loading are given Table 3. The current for model with 90mm stack length at rated power is equal to MEIC 13.5A and is 4 A larger one for model with 70 stack length. The flux density of stator pole for 90mm model is higher than 70mm model and but the iron loss is much lower. The efficiency of 90mm model that operates at MEIC 13.5A is about 3 points higher than the 70mm model.

The four models in Part 3.3 which have the same stack length 90mm are further analyzed using numerical simulation. The results are illustrated in Table 4 and Fig. 9. Table 4 shows that the efficiency is higher in winding design which have more turns per pole. However in the 90 turns model the back-emf exceeds the dc link voltage, so phase current decreases during conduction. Thus it is suggested to use more turns per winding while keeping the back-emf limit within limit.

Table 3. Performance comparison at rated power 2.2kW

Stack length (mm)	Iron loss (W)	Copper loss (W)	Flux Density (T)	Efficiency (%)
70	257.5	114.1	1.9	85.5
90	200.8	86.8	2.1	88.4

Table 4. Motor's performance according to windings

Turns per Pole	60	70	80	90
Wire diameter (mm)	1.63	1.45	1.45	1.29
Phase resistance (Ω)	0.275	0.405	0.463	0.658
Copper loss (W)	254.83	222.78	200.8	171.9
Iron loss (W)	86.67	84.71	86.8	92.41
Output power (W)	2110	2170	2200	2306
Efficiency (%)	86.1	87.6	88.4	89.7

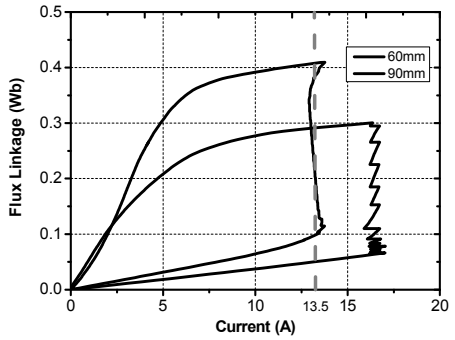

(a)

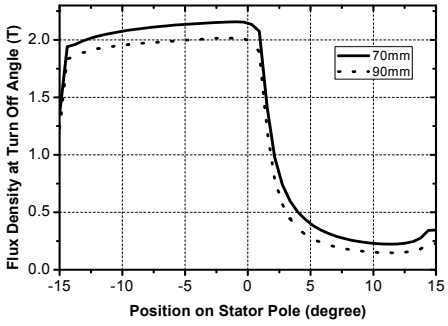

(b)

Fig. 8. Energy conversion loops: (a) and flux density along stator pole at turn off position; (b) for stack length 60 and 90 mm with the same turns per pole.

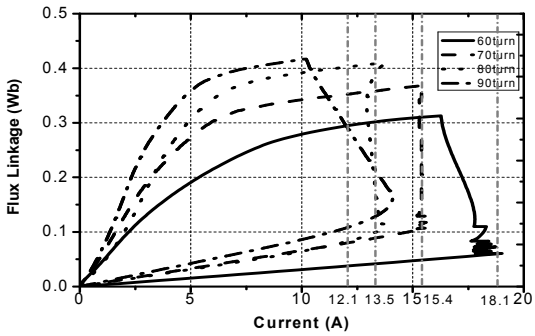

Fig. 9. Energy conversion loops with different windings and 90mm stack length operating at optimum point.

5.2. Experimental validation

The model with stack length 90mm and 90 turns per polewas manufactured and tested. The 3D model and photo of prototype are given in Fig. 10. The DC link voltage is 310V and the control algorithm is same as dynamic FEM simulation. The current waveforms from both experiment and simulation are shown in Fig.11, which shows good coherence. The mechanical losses were obtained by turning off the inverter at rated speed and the efficiency achieves 88.2% which excludes mechanical losses. This is a little lower than simulation result because of the losses in the inverter is not taken in to account in simulation.

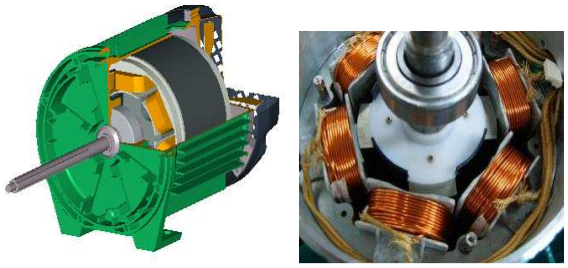

Fig.10. 3D model and photo of prototype

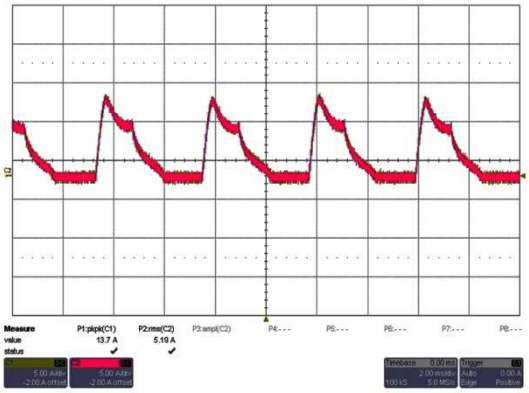

(a)

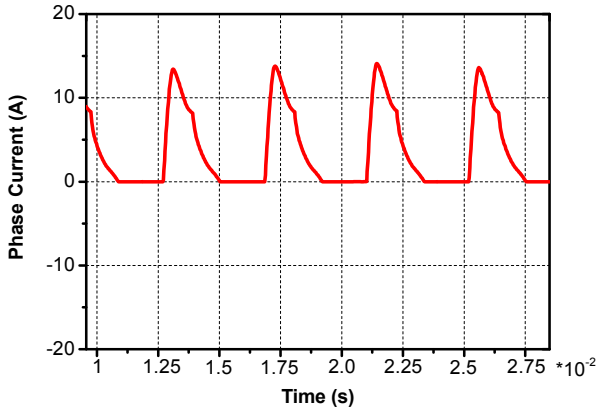

(b)

Fig.11. Comparison of phase current from experiment: (a) and dynamic FEM simulation; (b) results.

6. Conclusion

The optimization of energy conversion loop in switched reluctance motor for high efficiency is described for the first time in this paper. The maximum co-energy increment current (MEIC) was defined after modeling and analyzing the flux linkage curves. The variables during optimization were set as stack length and turns of winding. Then dynamic FEA simulation which can estimate the iron loss accurately was used to analyze the models with different stack length and turns per pole but same cross-section. Among these models the one which excited by MEIC has highest efficiency. Simulation result was also validated by experiment test. It could be concluded that Stack length varies with same winding in order to keep excitation current at MEIC for the rated power. The winding with more turns per pole cause high efficiency. But back-emf increases with turns so design with less turns is proper for high speed applications.

Appendix

Table 5. Motor's specifications and parameter

Item	Quantity
Stator outer diameter (mm)	150
Rotor outer diameter (mm)	80
Shaft diameter(mm)	24
Stack length (mm)	80
Stator yoke width (mm)	12.1
Rotor yoke width (mm)	13.2
Stator pole arc (degrees)	30
Rotor pole arc (degrees)	32
Air-gap length (mm)	0.4
DC voltage (V)	310
Rated Torque (N.m)	5.8
Rated Speed (rpm)	3600

References

[1] M. N. Anwar, I. Husain, A. V. Radun, A Comprehensive Design Methodology for Switched Reluctance Machines, IEEE Trans. Ind. Electron., 37 (2001) 1864-1892.

[2] Y. Hayashi, T. J. E. Miller, A New Approach to Calculating Core Losses in the SRM, IEEE Trans. on Ind. Appl., 31 (1995) 1039-1046.

[3] R. Krishnan, Switched Reluctance Motor Drives: Modeling, Simulation, Analysis, Design, and Applications. CRC, Boca Raton, 2001, pp. 79-120.

[4] S. H. Mao, M. C. Tsai, An analysis of the optimum operating point for a switched reluctance motor, Journal of Magnetism and Magnetic Materials, 282 (2004) 53-56.

[5] P. N. Materu, R. Krishnan, Estimation of Switched Reluctance Motor Losses, IEEE Trans. Ind. Appl., 28 (1992) 668-679.

[6] T. J. E. Miller, Optimal Design of Switched Reluctance Motors, IEEE Trans. Ind. Electron., 49 (2002) 15-27.

[7] A. V. Radun, Design Considerations for the Switched Reluctance Motor, IEEE Trans. Ind. Appl., 31 (1995) 1079-1087.

[8] N. K. Sheth, K. R. Rajagopal, Calculation of the flux-Linkage characteristics of a switched reluctance motor by flux tube method, IEEE Trans. Magn., 41 (2005) 4069- 4071.

[9] P. Vijayraghavan, PhD dissertation, Design of Switched

Reluctance Motors and Development of a Universal Controller for Switched Reluctance and Permanent Magnet Brushless DC Motor Drives, Virginia Polytechnic Institute and State University, Virginia, 2001.
[10] FLUX® 8.10 2D Application New features, Credat, France, 2003, pp. 63-70.

Acknowledgements

This research was financially supported by theMinistry of Education, Science Technology (MEST) and National Research Foundation of Korea(NRF) through the Human Resource Training Project for Regional Innovationn.

This research was also supported by Chinese National Science and Technology Major Project in the Twelfth Five-year Plan (2012ZX04001012).

Jian Li He received B.S degree in electrical engineering from Dalian University of Technology, Dalian, China, in 2005. He received M.S degree and PhD degree in electrical engineering from Dong-A University, Busan, Korea, in 2007 and 2011 respectively. Between 2011 and 2012, he was in a Post Doctor in Dong-A University. He joined the faculty of Huazhong University of Science and Technology, Wuhan, China in 2013 as Associate Research Professor in the College of Electrical and Electronic Engineering. His research interests include electrical machine and drives.

Ronghai Qu He received the B.E.E. and M.S.E.E. degrees from Tsinghua University, Beijing, China, in 1993 and 1996, respectively, and the Ph.D. degree in electrical engineering from the University of Wisconsin, Madison, in 2002. From 1996 to 1998, he was a Faculty Member of the Electrical Engineering Department, Tsinghua University, and in 1998, he was with the Wisconsin Electric Machines and Power Electronics Consortium as a Research Assistant. He was a Senior Electrical Engineer with Northland, a Scott Fetzer Company, in 2002, and from 2003 to 2010, he was with the General Electric (GE) Global Research Center, Niskayuna, NY, where he was a Senior Electrical Engineer with the Electrical Machines and Drives Laboratory. He is currently a Professor with the College of Electrical and Electronic Engineering, Huazhong University of Science and Technology, Wuhan, China. His research interests include permanent magnet machines and drives, superconducting electric machines, and wind power generation. Dr. Qu has authored 24 published technical papers and is the holder of 32 U.S. patents/patent applications. He is a full member of Sigma Xi. He has been the recipient of several awards from GE Global Research Center since 2003, including the Technical Achievement and Management Awards. He is also the recipient of the 2003 and 2005 Best Paper Awards, third prize, from the Electric Machines Committee of the IEEE Industry Applications Society for presentations at the 2002 and 2004 IAS Annual Meeting, respectively. He has been listed in Marquis Who's Who in America since 2007.

Zhichu Chen He received B.S degree in Electrical Engineering and Automation from Southwest Jiaotong University. Since 2005, he has been with CSR Zhuzhou Electric Locomotive Research Institute Co., Ltd, Hunan Province, China. His current research interests include analysis and optimazation design of electric motors.

Yun-Hyun Cho He received his M. Eng. and D. Eng. in Electrical Engineering from Han-Yang University, Seoul, Korea, in 1986 and 1991, respectively. From 1990 to 1995, he was a Senior Researcher at Korea Electrotechnology Research Institute (KERI). In 1995, he joined Dong-A University, Department of Electrical Engineering, as Professor. His field of interest is electrical machine and power electronics.